



Accuracy of full-arch digital impressions: an in vitro and in vivo comparison

Christine Keul¹ · Jan-Frederik Güth¹

Received: 11 January 2019 / Accepted: 16 May 2019 / Published online: 27 May 2019
© Springer-Verlag GmbH Germany, part of Springer Nature 2019

Abstract

Objectives Comparison of full-arch digital impressions to conventional impressions in vitro and in vivo.

Materials and methods A straight metal bar was fixed between the second upper molars as a reference structure in the mouth of a voluntary patient and a corresponding polymer model. The following digitalization methods were applied: (1) the maxilla was digitized in vivo 12 times with the iTero Element (P-SCAN); (2) the maxilla was captured in vivo 12 times by conventional impression and the impression was digitized by a desktop scanner (P-IMP); (3) the impressions were poured and the 12 referring gypsum master-casts were scanned with the same desktop scanner (P-CAST); (4) the polymer model was digitized in vitro 12 times with the iTero Element (M-SCAN); (5) the polymer model was captured in vitro 12 times by conventional impression and the impression was digitized by a desktop scanner (M-IMP); (6) the impressions were poured and the 12 referring gypsum master-casts were scanned with the same desktop scanner (M-CAST). Datasets were exported and metrically analyzed (Geomagic Control X) to determine three-dimensional length aberration and angular distortion versus the reference structure. Mann–Whitney *U* test was implemented to detect differences ($p < 0.05$).

Results For multiple accuracy parameters, P-SCAN and M-SCAN showed similar or superior results compared to the other digitalization methods. The following length deviations were found: M-SCAN (– 55 to 80 μm), M-IMP (110 to 329 μm), M-CAST (88 to 178 μm), P-SCAN (– 67 to 76 μm), P-IMP (125–320 μm), and P-CAST (92–285 μm).

Conclusions Within the limitations of this study, the iTero-scan seems to be a valid alternative to conventional impressions for full arches.

Clinical relevance Intraoral scanners are more and more used in daily routine; however, little is known about their accuracy when it comes to full-arch scans. Under optimum conditions, the direct digitalization using the iTero Element intraoral scanning device results in the same and for single parameters (arch width and arch distortion) even in higher accuracy than the indirect digitalization of the impression or the gypsum cast using a desktop scanner.

Keywords Digital impression · Accuracy · Full-arch impression · iTero Element · Metrology analysis

Introduction

Intraoral scanning supplements more and more the well-established conventional impressions using elastomers and the subsequent indirect digitalization of the impressions itself or the resulting casts. Therefore it can be meanwhile

considered as a common entry to dental computer-aided design/computer-aided manufacturing (CAD/CAM) processes [1]. Virtual models are the basis for all steps in the digital workflow that enables a wide range of innovative diagnosis and rehabilitation options for a patient-centered treatment [2–4].

The available intraoral digitalization systems are working on optical measuring principles [5, 6] to digitize the intraoral structures directly in the patient's mouth [7, 8]. This avoids different working steps, like the selection of the proper impression tray, application of the adequate impression technique, disinfection, transport, and fabrication of dental gypsum casts. Besides the understandable enthusiasm for intraoral

✉ Christine Keul
Christine.keul@med.uni-muenchen.de

¹ Department of Prosthodontics, LMU Munich, Goethestraße 70, 80336 Munich, Germany

scanning, currently a strong focus is on the accuracy of the resulting datasets. Today literature is contradictory due to different methodologies, analyses, different scanning systems, and multiple ways of data interpretation.

Some literature focuses on the accuracy of single-tooth scans or on areas up to one quadrant [5, 7, 9, 10] and shows that the process of direct digitalization resulted in equivalent or even higher accuracy for digitizing single teeth or hemi-arches [5, 7, 11]. Other studies report on full-arch implant scans [12–15] and showed likewise equivalent or even higher accuracy for direct digitalization [14]. Other researchers investigated full-arch direct digitalization by an *in vitro* test design on basis of best-fit dataset alignment and found contradictory results in regard to the accuracy [6, 16–19]. Further on, also the latest *in vivo* studies apply mostly a best-fit alignment of datasets to evaluate the accuracy of full-arch scans [20–23] and still show inhomogeneous patterns and results.

Regarding clinical accuracy studies, a major problem is to generate a highly accurate reference dataset of the clinical situation because the clinical patient might not be digitized by a tactile, radiological, or high-precision industrial optical scanning device [1]. So the before mentioned studies [20–23] only compared the reproducibility, meaning the precision of direct and indirect digitalization, but not the accuracy in sense of trueness and precision as defined in ISO 5725-1:1994 [24] that limits the interpretation of the results. Another limitation regarding the analysis is the superimposition procedure itself and the subsequent interpretation of differences: Due to the methodology of dataset alignment and calculating the mean difference between the dataset surfaces, the results also might be influenced by the superimposition algorithm of the metrology software [8].

To overcome these drawbacks, an innovative methodology was developed and already applied *in vitro* to measure reference geometries for the determination of the accuracy of full-arch scans without the need of dataset superimposition [8]. This enables to measure “real” length differences, linear position shifts, and angles. The aim of the present study was to further develop the mentioned *in vitro* methodology to apply it *in vivo* and compare the results to indirect digitalization. Further on, the differences between *in vitro* scans and *in vivo* scans should be evaluated using the same scanner.

The null hypotheses were that according the trueness and precision:

1. There will be no quantitative differences between direct and indirect digitalization, and
2. There will be no differences between the scans conducted *in vivo* and *in vitro*.

Materials and methods

As a basis for the study, a voluntary patient has participated for the *in vivo* measurement. For the *in vitro* part, an impression of the maxilla of the same patient was taken (Aquasil Ultra DECA Monophase LOT 170503) and casted with a model resin (AlphaDie MF, LOT 2012008441; Schütz Dental GmbH). On the basis of this model, an absolutely straight metal bar (GARANT, DIN 875-00-g; Hoffmann Group) was adapted that connected the second molars of the left and right hemi-arch and fitted in the patient’s mouth as well as on the resin model. Figure 1 depicts the study design. The study was approved by the Ethics Committee (511–14), registered at the German Clinical Trial Register (DRKS: 00015459) and performed in accordance with the ethical standards of the institutional research committee and with the 1964 Helsinki declaration. Before starting the data acquisition, the voluntary patient signed an informed consent. Furthermore, pilot tests with the iTero Element were conducted and no negative influence of the reflective metal bar could be observed.

Acquisition of the reference dataset of the bar

A reference dataset of the metal bar was generated using a coordinate measuring machine (Mitutoyo Crysta Apex C 574; Createch Medical; MCOSMOS Mitutoyo Software; Mitutoyo) at a temperature of 20 °C with the following specifications: MPEe 1.9 µm + (3*L/1000). The dataset was exported and converted into STL data (surface tessellation language). The reference dataset was analyzed with the same methodology like the test datasets, as described below.

Acquisition of virtual test model data

For the *in vitro* part of the study, the metal bar was attached on the resin model, using provisional resin material (Clip F; Voco GmbH) to ensure a fixed position and digital impressions were carried with the intraoral scanning device (iTero Element S/N RTC2016W46A005 and 42853; Align Technology), using the following defined scanning strategy (group M-SCAN, $n = 12$): startpoint occlusal on tooth 27, moving toward 17, turning to palatal side and moving back to 27, turning to buccal side and moving to 17, finally turning to occlusal surface and moving back to 27.

Furthermore, 12 conventional impressions were made by means of a high-precision impression material (Aquasil Ultra DECA Monophase LOT 170503 and Aquasil Ultra XLV cartridge, LOT 170616; DensplySirona) and individually produced impression trays (Palatray XL, LOT 132651; Heraeus Kulzer). Therefore, the bar was attached (Clip F) and undercuts of the bar were blocked. After each impression, the bar

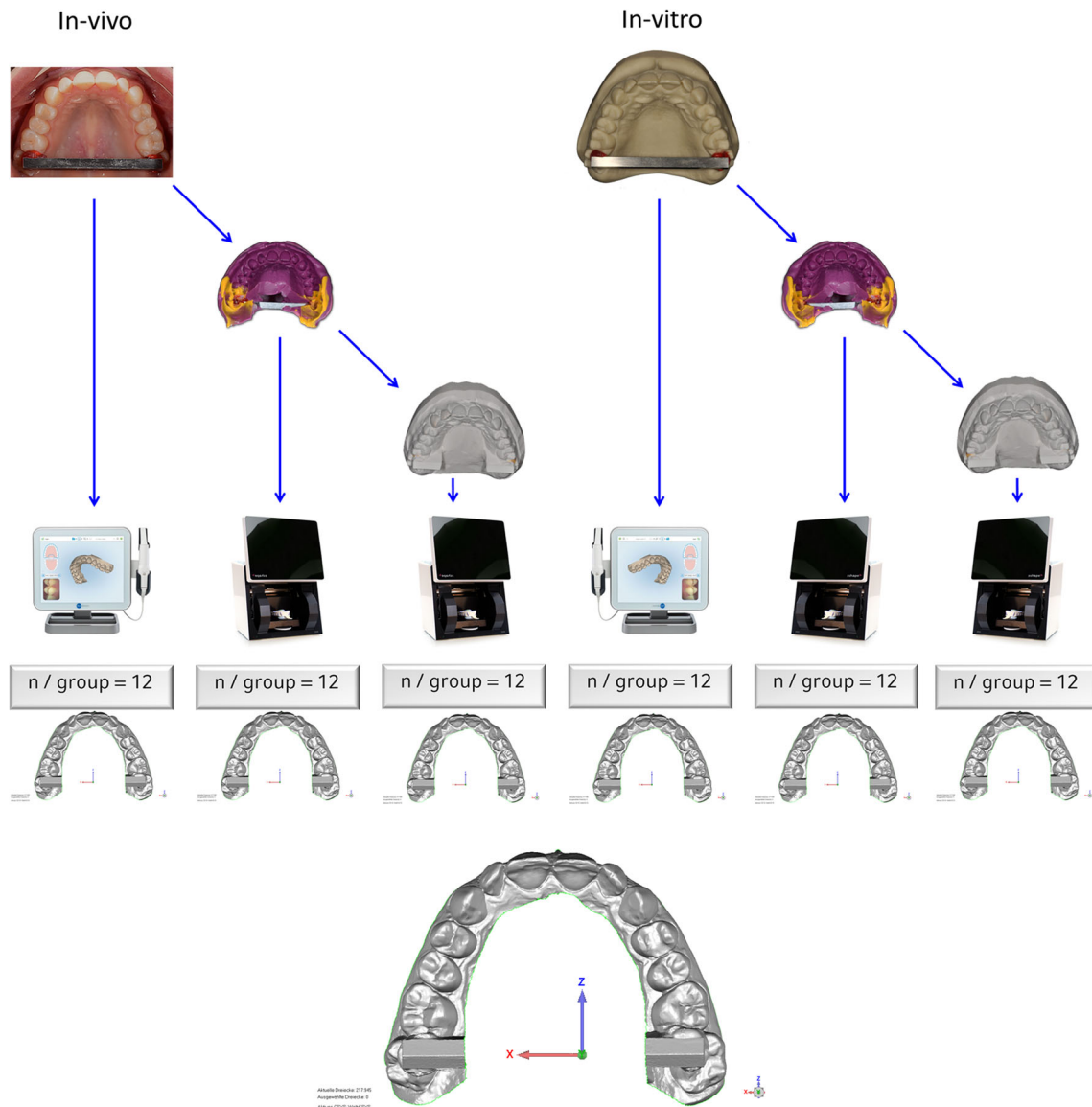


Fig. 1 Study design with test groups and orientation of the virtual model

was carefully removed from the impression. According to clinical procedures, the impressions were visually controlled for possible defects in the area of the bar, stored for 2 min in a disinfection bath (ORBI-sept Abformdesinfektion, LOT A0984; Orbis Dental Handelsgesellschaft mbH) and digitized after 24 h (group M-IMP, $n = 12$) with a laboratory scanner (D810, Dental Manager 2013-1; 3shape). Subsequently, plaster models were manufactured (Plurastone white, LOT A0984; Pluradent) and digitized 24 h after casting (M-CAST, $n = 12$), using the same laboratory scanner.

For the in vivo part, the bar was temporarily attached to the occlusal surfaces of the patient’s second molars using Clip F to ensure a fixed position before the digital and conventional impressions were taken. After fixation of the bar, intraoral digital impressions of the maxilla (iTero Element; Align

Technology) were taken, using the given defined scanning strategy (P-SCAN, $n = 12$).

Furthermore, 12 conventional impressions are made by means of a high-precision impression material (Aquasil Ultra DECA Monophase LOT 170503 and Aquasil Ultra XLV cartridge, LOT 170616; DensplySirona) and individually produced impression trays (Palatray XL, LOT 132651; Heraeus Kulzer). Therefore, the bar was attached (Clip F) in the patient’s mouth and undercuts of the bar were blocked. After each impression, the bar was carefully removed from the impression. The impressions were visually controlled for possible defects in the area of the bar and stored for 2 min in a disinfection bath (ORBI-sept Abformdesinfektion, LOT A0984; Orbis Dental Handelsgesellschaft mbH) and digitized after 24 h (P-IMP, $n = 12$) with the same laboratory scanner. Subsequently plaster models were manufactured (Plurastone

white, LOT A0984; Pluradent) and digitized 24 h after casting (P-CAST, $n = 12$), using the same laboratory scanner.

Data analysis

The reference dataset from the CMM (coordinate measuring machine) and all obtained test datasets were measured by metrology software (Geomagic Control X; Geomagic) by constructing surface areas on the bar using the “contact feature mode.”

In the first quadrant, the features anterior plane (A1), posterior plane (P1), and vestibular plane (V1) were constructed on the outside of the bar. In the second quadrant, the features anterior plane (A2), posterior plane (P2), and vestibular plane (V2) were constructed on the other outside of the bar (Fig. 2).

From the intersections of the anterior and posterior planes for each quadrant, one line resulted on the edge of the bar (first quadrant, L1; second quadrant, L2).

The intersection of the L1 with plane V1 and L2 with the plane V2 defined the points VL1 and VL2, respectively.

The plane V2 was parallel shifted by 55.066 mm (reference length of the bar) in the direction of the first quadrant, resulting in plane V2' to construct the point VL2'.

Calculation of the parameters

The following parameters of the constructed points and lines were used for the further calculation:

- Lowercase letters, the x , y , z coordinates of the points: $x_{point\ name}$, $y_{point\ name}$, $z_{point\ name}$
- Capital letters, the X , Y , Z vector direction of the lines: $X_{line\ name}$, $Y_{line\ name}$, $Z_{line\ name}$

Reference dataset

The reference length of the metal bar in the virtual datasets (R) was calculated between VL1 and VL2, using the x , y , and z coordinates of both points and set on 55.066 mm using Formula 1.

$$R = \sqrt{(x_{VL2} - x_{VL1})^2 + (y_{VL2} - y_{VL1})^2 + (z_{VL2} - z_{VL1})^2}$$

Additionally, the bar was analyzed for possible angular deviations using Formula 2.

$$\alpha_{overall} = \text{acos} \frac{X_{L1} \cdot X_{L2} + Y_{L1} \cdot Y_{L2} + Z_{L1} \cdot Z_{L2}}{\sqrt{X_{L1}^2 + Y_{L1}^2 + Z_{L1}^2} \cdot \sqrt{X_{L2}^2 + Y_{L2}^2 + Z_{L2}^2}} \cdot \frac{180}{\pi}$$

Using this formula, the calculated angle deviation value of both ends of the metal bar was 0.01°.

Test datasets

The length of the metal bar in the test datasets (L) was calculated between VL1 and VL2, using the x , y , and z coordinates of both points and Formula 1, given above.

To determine the aberration of the linear arch width, the difference value (ΔL) to the reference bar length (R) was calculated by:

$$\Delta L = L - R$$

To distinguish in which three-dimensional axis the linear width difference occurred, the vectorial error (VE) as linear parameter was determined and differentiated in values for the X -, Y -, and Z -axis (Fig. 1). The length of VE was then calculated between point VL2' and VL2 and the linear shift in the X -, Y -, and Z -axes using the following formulas:

$$VE = \sqrt{(x_{VL2} - x_{VL2'})^2 + (y_{VL2} - y_{VL2'})^2 + (z_{VL2} - z_{VL2'})^2}$$

$$\begin{matrix} VE(x) \\ VE(y) \\ VE(z) \end{matrix} = \begin{pmatrix} x_{VL2} - x_{VL2'} \\ y_{VL2} - y_{VL2'} \\ z_{VL2} - z_{VL2'} \end{pmatrix}$$

To determine the angular warpage between both hemi-arches, the overall angle ($\alpha_{overall}$) between L1 and L2 was calculated using the Formula 2, given above.

To distinguish the projection of the angle in coronal and horizontal direction, $\alpha_{overall}$ was mathematically projected on the X - Y plane ($\alpha_{coronal}$) and the X - Z plane ($\alpha_{horizontal}$):

$$\alpha_{coronal} = \text{acos} \frac{X_{L1} \cdot X_{L2} + Y_{L1} \cdot Y_{L2}}{\sqrt{X_{L1}^2 + Y_{L1}^2} \cdot \sqrt{X_{L2}^2 + Y_{L2}^2}} \cdot \frac{180}{\pi}$$

$$\alpha_{horizontal} = \text{acos} \frac{X_{L1} \cdot X_{L2} + Z_{L1} \cdot Z_{L2}}{\sqrt{X_{L1}^2 + Z_{L1}^2} \cdot \sqrt{X_{L2}^2 + Z_{L2}^2}} \cdot \frac{180}{\pi}$$

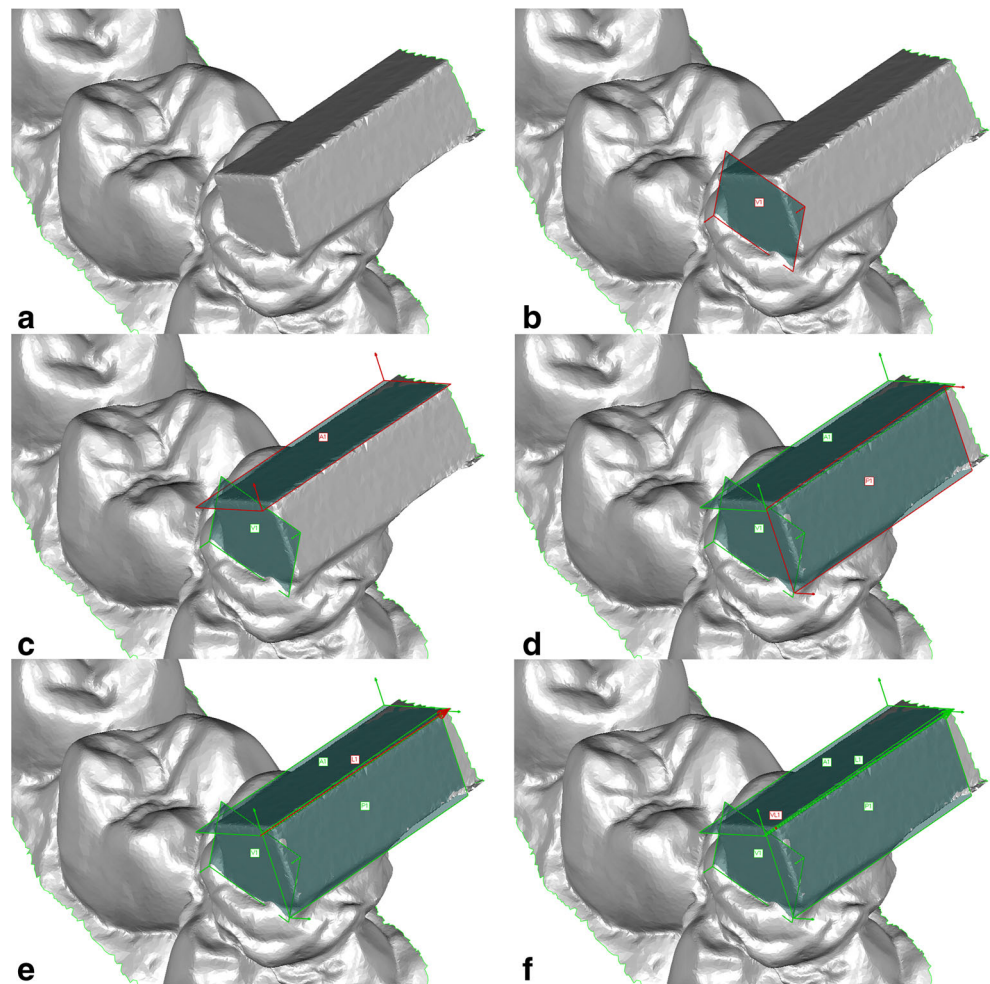
Statistics

For data analysis, the Statistical Package for the Social Science version 25 (SPSS Inc.) was used. The level of significance was set at 5% ($p < 0.05$). Descriptive statistics (mean, standard deviation, median, and 95% confidence intervals) were calculated for all parameters. Normality of data distribution was tested using Kolmogorov–Smirnov and Shapiro–Wilk test. Statistical differences for the measured parameters were determined by Mann–Whitney U test.

Results

The descriptive statistic of the measured linear and angular parameters is given in Table 1. Kolmogorov–Smirnov test

Fig. 2 Construction of features on the metal bar in the first quadrant. **a** Metal bar without features, **b** vestibular plane (V1) on metal bar, **c** anterior plane (A1) on metal bar, **d** posterior plane (P1) on metal bar, **e** intersection line of anterior and posterior plane (L1), **f** intersection point of vestibular, anterior, and posterior lines (VL1)



revealed that 17 of 48 parameters were not normally distributed. Boxplots in Figs. 3, 4, and 5 depict the measured values graphically.

Determination of trueness

Impact of digitalization method

Regarding the *in vitro* results, no significant differences were found between different ways of digitalization for the parameters VE, VE(y) and VE(z), α_{overall} , α_{coronal} , and α_{axial} . For the parameters ΔL and VE(x), the method of direct digitalization (M-SCAN) resulted in significantly better values, followed by indirect digitalization of the gypsum cast (M-CAST). The method of indirect digitalization of the impression (M-IMP) resulted in the significant highest deviation.

Regarding the *in vivo* results, no significant differences were found between different ways of digitalization for the parameters VE, VE(y), VE(z), and α_{axial} . For the linear parameters ΔL and VE(x), the method

of direct digitalization (P-SCAN) resulted in significantly better values, followed by indirect digitalization of the gypsum cast (P-CAST). The method of indirect digitalization of the impression (P-IMP) resulted in the significantly highest deviation. For the angular parameters α_{overall} and α_{coronal} , the significant best values were obtained by direct digitalization (P-SCAN), while the indirect digitalization of the impression (P-IMP) resulted in the highest deviation.

Impact of the scanning object (in vivo vs. in vitro)

For the method of direct digitalization, no differences between the *in vitro* and *in vivo* results were found for the parameters ΔL , VE, VE(x), VE(y), and α_{overall} . For the parameters VE(z) and α_{axial} , the *in vitro* results showed significantly better values than *in vivo* results, while for the parameter α_{coronal} , significantly better values were observed for the *in vivo* results.

For the method of indirect digitalization of the impression, no differences between the *in vitro* and *in vivo*

Table 1 Measuring values of the study

		ΔL (μm)	VE (μm)	VE(x) (μm)	VE(y) (μm)	VE(z) (μm)	α_{overall} ($^{\circ}$)	α_{coronal} ($^{\circ}$)	α_{axial} ($^{\circ}$)
Results in vitro									
Direct digitalization M-SCAN	MW	4.2	287.4	43.8	238.1	21.0	0.46	0.45	0.73
	SD	44.4	88.4	154.7	88.5	41.8	0.11	0.12	0.04
	Min	-55.0	185.9	-51.7	17.2	-42.1	0.23	0.20	0.02
	Med	-8.6	272.1	-5.7	252.7	20.6	0.48	0.48	0.07
	Max	80.0	525.0	520.5	327.2	108.8	0.58	0.58	0.13
	95% CI	-23.9	231.1	-54.4	181.8	-5.5	0.39	0.37	0.04
	Statistics	A/a	A/a	*/A/a	A/a	A/a	A/a	B/a	A/a
Indirect digitalization of the impression M-IMP	MW	200.0	318.3	188.0	200.7	51.0	0.38	0.37	0.09
	SD	62.7	150.8	72.0	154.0	137.9	0.13	0.12	0.07
	Min	110.6	108.8	51.9	3.1	-85.6	0.17	0.17	0.01
	Med	191.4	291.8	190.9	179.0	-9.4	0.40	0.38	0.07
	Max	329.3	622.0	310.5	500.2	351.7	0.61	0.55	0.26
	95% CI	160.1	222.4	142.2	102.8	-36.5	0.30	0.29	0.04
	Statistics	A/c	A/a	A/c	A/a	*/A/a	A/a	A/a	A/a
Indirect digitalization of the gypsum cast M-CAST	MW	113.4	256.7	114.0	215.3	6.7	0.42	0.41	0.08
	SD	23.4	159.2	23.4	167.3	61.6	0.36	0.36	0.05
	Min	88.2	93.6	87.4	33.3	-114.5	0.17	0.15	0.01
	Med	109.5	204.1	109.8	167.3	22.3	0.28	0.28	0.07
	Max	178.4	596.4	179.1	576.7	108.2	1.33	1.32	0.18
	95% CI	98.5	155.5	99.1	108.8	-32.4	0.18	0.17	0.05
	Statistics	*/A/b	*/A/a	A/b	*/A/a	A/a	*/A/a	*/A/a	A/a
Results in vivo									
Direct digitalization P-SCAN	MW	8.0	305.1	8.1	219.9	-170.2	0.40	0.30	0.22
	SD	51.4	157.1	50.8	110.1	164.7	0.14	0.14	0.15
	Min	-67.0	130.3	-65.2	445.1	-605.4	0.20	0.09	0.00
	Med	26.4	294.7	26.5	231.3	-136.0	0.36	0.26	0.20
	Max	76.5	753.4	78.5	445.1	7.3	0.58	0.54	0.56
	95% CI	-24.7	205.2	-24.2	149.9	-274.7	0.31	0.20	0.12
	Statistics	A/a	*/A/a	A/a	A/a	*/B/a	A/a	A/a	B/a
Indirect digitalization of the impression P-IMP	MW	209.2	412.8	208.8	293.9	-46.5	0.82	0.77	0.24
	SD	59.9	185.3	59.1	238.6	125.0	0.45	0.39	0.27
	Min	125.1	198.2	127.9	-175.5	-368.7	0.30	0.30	0.02
	Med	186.3	351.2	184.1	264.6	-19.5	0.77	0.74	0.18
	Max	320.3	739.1	323.9	648.2	102.6	1.80	1.50	1.01
	95% CI	171.0	295.0	171.2	142.2	-125.9	0.53	0.51	0.06
	Statistics	*/A/c	A/a	*/A/c	A/a	*/A/a	B/b	B/b	A/a
Indirect digitalization of the gypsum cast P-CAST	MW	142.7	517.0	142.8	276.5	139.2	0.91	0.77	0.45
	SD	57.1	627.6	57.6	247.8	702.9	1.27	0.90	0.92
	Min	92.95	129.0	93.4	23.2	-398.1	0.16	0.15	0.01
	Med	130.2	268.0	129.7	211.7	-5.7	0.67	0.65	0.16
	Max	285.1	2349.9	288.1	896.1	2332.7	4.84	3.52	3.32
	95% CI	106.4	118.2	106.2	119.0	-307.4	0.11	0.19	0.14
	Statistics	A/b	*/A/a	A/b	A/a	*/A/a	*/A/ab	*/A/ab	*/A/a

MW = mean, SD = standard deviation, Min = minimum, Med = median, Max = maximum, CI = 95% confidence interval

*Not normally distributed

A, B, C = differences between model and patient

a, b, c = differences of digitalization type

results were found for the parameters ΔL , VE, VE(x), VE(y), VE(z), and α_{axial} . For the parameters α_{overall} and α_{axial} , the in vitro results showed significantly better values than in vivo results.

For the method of indirect digitalization of the cast, no differences were found between the in vitro and in vivo results for all measured parameters.

Determination of precision

Impact of digitalization method

Within in vitro results for six of eight measuring parameters, the lowest standard deviation—and therefore the highest precision—was found for the method of direct digitalization.

Within in vivo results for seven of eight measuring parameters, the lowest standard deviation—and therefore the highest precision—was found for the method of direct digitalization.

Impact of the scanning object (in vivo vs. in vitro)

For the direct digitalization for seven of eight measuring parameters, a lower standard deviation—and therefore a better precision—was found for the in vitro results.

For the indirect digitalization of the impression for five of eight measuring parameters, a lower standard deviation—and therefore a better precision—was found for the in vitro results.

For the indirect digitalization of the gypsum cast for all measuring parameters, a lower standard deviation—and therefore a better precision—was found for the in vitro results.

Discussion

The present study is based on a linear reference object that can be used for in vitro and in vivo analysis to determine the accuracy of different ways for a full-arch digitalization. To the authors’ knowledge, this is the first approach to compare the accuracy of digitalization processes carried out in vitro and in vivo using the same reference object. In consequence, not

only the influence of the digitalization type could be investigated but simultaneously also the influence of the in vivo environment. Hereby the influence of the intraoral conditions like limited space for the optical digitalization unit, possible fogging of the digitalization unit, the movement of the patient, the intraoral illumination, and the humidity due to saliva could be observed. All these factors have been mentioned to have an impact on the precision of the scanning results [21]. For the present study, the upper dental arch was used. This might lead to better values as part of the palate can be scanned additionally and can be utilized as additional frame for the matching of the single pictures [1]. Further on, the maxilla presents no distortion during opening in comparison to the mandible [25]. Generally, the straight bar could not be fixed sufficiently in the mandible due to the tongue.

The first null hypothesis, stating that no differences regarding the accuracy will occur due to different digitalization types, has to be rejected. Regarding the in vitro results for the trueness, the linear parameters ΔL and $VE(x)$ resulted in significantly highest trueness for the method of direct digitalization (M-SCAN), while the indirect digitalization of the impression (M-IMP) resulted in the significantly worst trueness. Only within the in vivo results the angular parameters $\alpha_{overall}$ and $\alpha_{coronal}$ showed the significantly highest trueness for the direct digitalization (P-SCAN), while the indirect

Fig. 3 Boxplots of the parameter length deviation ΔL

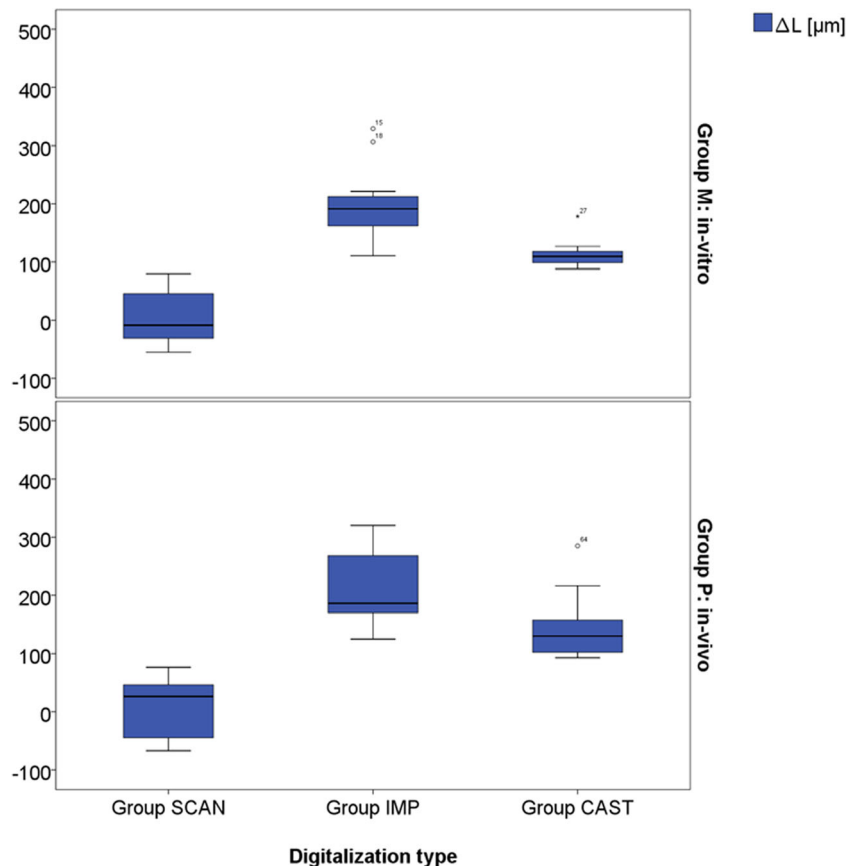
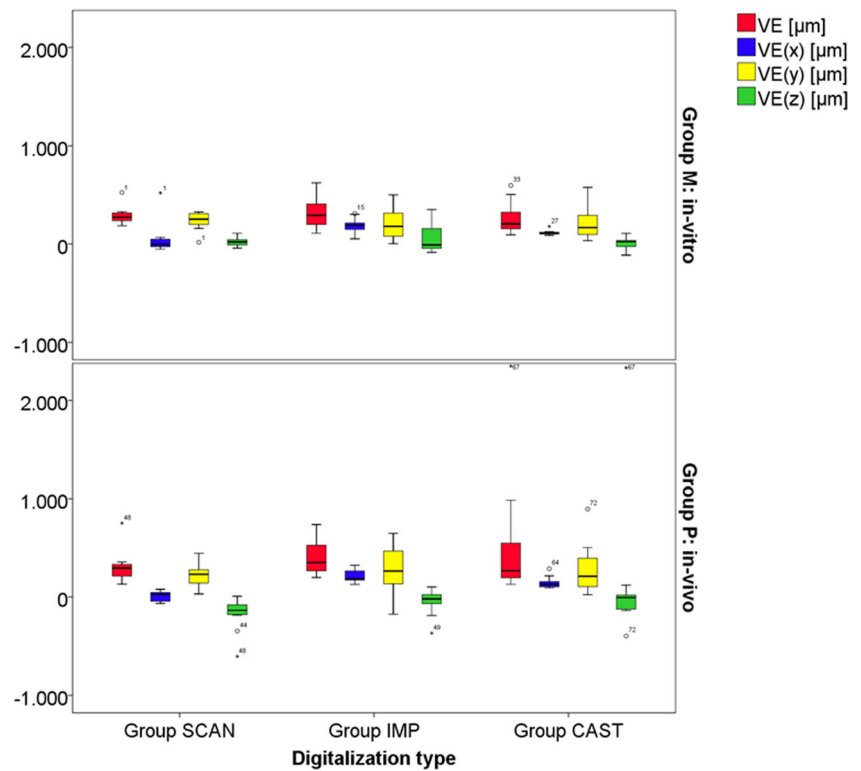


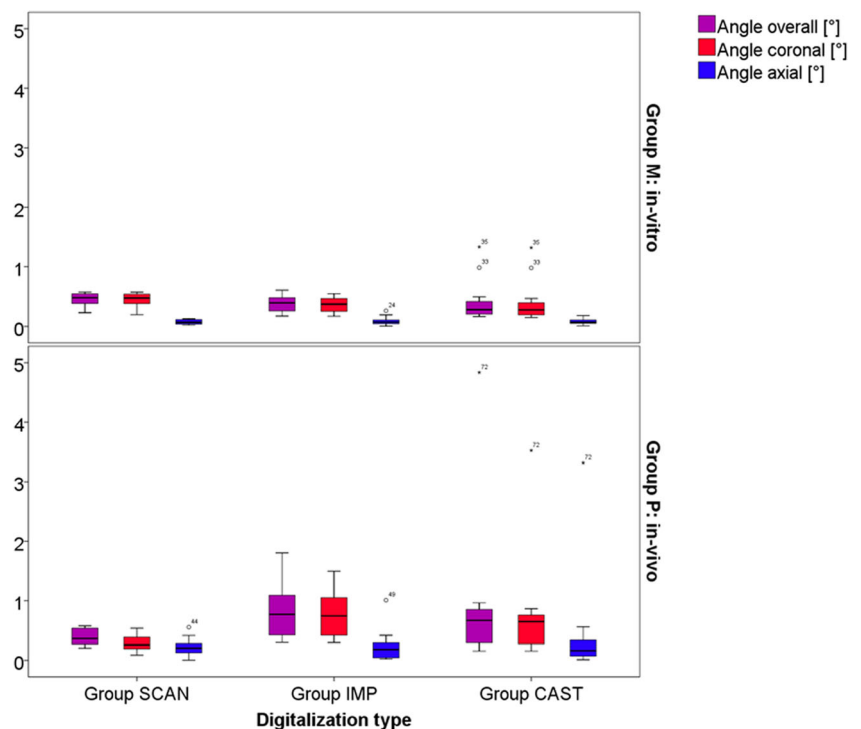
Fig. 4 Boxplots of the linear parameters VE, VE(x), VE(y), VE(z)



digitalization of the impression (P-IMP) showed the worst trueness. For the in vivo and in vitro precision, most of the measuring parameters resulted in the lowest standard deviation—and therefore the best precision—for the method of direct digitalization. This observation is in contrast to prior

study results on the basis of the method of measuring real geometries [1]. Additionally, other in vitro and in vivo studies on the basis of best-fit dataset alignment stated contradictory results in view of accuracy [6, 16–23]. The digital and conventional impressions resulted on the basis of an upper jaw

Fig. 5 Boxplots of the angular parameters $\alpha_{overall}$, $\alpha_{coronal}$, and α_{axial}



reference model from cobalt–chromium alloy in similar values for trueness (LAVA C.O.S. $40.3 \pm 14.1 \mu\text{m}$, CEREC Bluecam $49 \pm 14.2 \mu\text{m}$, conventional impression $55 \pm 21.8 \mu\text{m}$) and precision (LAVA C.O.S. $60.1 \pm 31.3 \mu\text{m}$, CEREC Bluecam $30.9 \pm 7.1 \mu\text{m}$, conventional impression $61.3 \pm 17.9 \mu\text{m}$) [6]. In contrast, digital impressions were significantly less accurate with a precision of $32.4 \pm 9.6 \mu\text{m}$ and a trueness of $58.6 \pm 15.8 \mu\text{m}$ than conventional impressions with a precision of $12.5 \pm 2.5 \mu\text{m}$ and a trueness of $20.4 \pm 2.2 \mu\text{m}$ on the basis of the same evaluation methodology [19]. Full-arch digitalization with the iTero Element was depicted to be less accurate than scanning the gypsum cast with the D250 desktop scanner [21]. However, a direct comparison of these values is difficult due to the different study setups, methodology, and software versions.

Especially for full-arch fixed dental restorations, the linear and angular warpage of the digital and/or conventional impression is a crucial factor that might lead to misfitting dental restorations. The clinical consequences might be even worse in implant-supported full-arch restorations due to the rigid osseointegration of implants [26]. Further on, angular aberrations in the coronal plane may result in a unilateral imperfect static and dynamic occlusal relation. Angular aberrations in the axial plane may result in aberrations in the occlusal plane in form of posterior/anterior or lateral deviations.

The second null hypothesis, stating that no differences regarding the accuracy will occur between the *in vitro* and *in vivo* results, also has to be rejected as mainly the angular parameters showed better accuracy for *in vitro* data acquisition. This is in accordance with prior literature, stating the extraoral digitalization of the patient's model with the iTero Element was more accurate than the *in vivo* digitalization [21]. In general, the intraoral digitalization of the metal bar fixed on top of the teeth was particularly challenging due to the limited space in the posterior area of the arch. So the practitioner for the ascertainment of the virtual datasets was specially trained to make sure that the datasets were complete. As a limitation, it may be questionable if the scanning strategy may have an influence on the accuracy as—due to the dimension of the applied metal bar—the focal distance of the optic was not optimal. Also, for the conventional impressions, the material retained stronger in the proximal area of the natural teeth than on the resin model, which may result in a higher distortion for the *in vivo* impression.

The results of the linear parameters resulted for the *in vitro* and the *in vivo* data both in negative and in positive values. According to the orientation in the three-dimensional space, the *x*-axis corresponds to the lateral axis, the *y*-axis to the long axis in cranial direction, and the *z*-axis to the sagittal axis in anterior direction (Fig. 1). Prior to the statistical analysis for the determination of significant differences in view of the accuracy, all linear parameters need a transformation to become positive. Therefore, all values were added by $1000 \mu\text{m}$

to enable statistical analysis by Mann–Whitney *U* test. For determination of the trueness, the real measured values were used and compared to a reference measurement of the bar by CMM. The CMM has according to the manufacturer a measurement accuracy of $\text{MPE}_e = 1.9 \mu\text{m} + (3 \cdot L/1000)$, where *L* is the real length of the bar. This means that the accuracy was $2.07 \mu\text{m}$ over the complete length of the metal bar. For determination of the precision of the different digitalization methods, the standard deviation of the measured values was used.

The linear reference object of the present study facilitates the analysis of linear and angular parameters of virtual three-dimensional datasets from different digitalization methods. In difference to other literature, the fixation of the reference structure on top of the teeth was not so demanding [1] due to the fact that only one single and stable structure had to be fixed, and not different reference objects to be in correct three-dimensional distance to each other. Several studies used geometrical structures for investigating full-arch accuracy before [27–30], but only scant studies investigate additionally to the linear distances the angular parameters [1, 8]. Due to the possible deformation of the impression material, the removing of the bar from the impressions may be one limitation of the present study. As during the study no continuous increase of the measurement values could be observed, no significant influence of the described operations could be assumed. Therefore, the deforming influence of removing the bar should not be of decisive character.

Different studies dealing with dimensional accuracy of virtual datasets used the superimposition of the test datasets with a highly accurate reference dataset [6, 18, 22]. By investigating the complete surface of the three-dimensional dataset, the spatial differences can be calculated for every point of the dataset. However, the different metrology software versions are working with different best-fit algorithms for the superimposition of datasets. Hence, different software providers or different software updates may result in different spatial values for the calculation process. The best-fit alignment can also disguise distortions in the dataset by positioning the test data in an optimal position to the reference data over the complete model surface [1]. Penetrations of the virtual datasets due to the positive and negative spatial deviations result in values close to zero when calculating the mean values. Apart from the superimposition process to determine the accuracy of datasets, the geometrical measurement of incorporated reference structures can be used for the analysis. The use of these geometrical structures has the advantage that the dimensions of the structure can be determined before the digitalization process by using CMM as a highly accurate measurement process. Therefore, the advantage of the present study design was that no superimposition was needed for the dimensional analysis of data.

The only comparable study used an in vitro study design and stated for a different intraoral scanner—working on the basis of active wavefront sampling (True Definition)—significantly lower values for single linear measuring parameters, as well as for single angular parameters than for the indirect digitalization of the gypsum cast [8]. However, this study was based only on the evaluation of direct digitalization and indirect digitalization of a cast. The present study also investigated the digitalization of the impression itself as only limited literature could be found instigating the accuracy of full-arch impression scanning. The accuracy of simulated clinical crown preparations in a full arch by digitalization of the impression itself and the gypsum cast varies with the shape of the scanned surface [31]. For the model size of a hemi-arch with three implants, the digitalization of the impression resulted in the highest accuracy [32]. This is in contrast to the present results where the digitalization of the impression resulted in the worst values for the parameters ΔL and $VE(x)$ both in vitro and in vivo. The design of the full-arch model for the present study is based on naturally shaped teeth with a natural curvature and natural undercuts. Although for the indirect digitalization of the impression special holding devices are available, undercuts in the impression are a problem for the optical digitalization process. Despite the impression is scanned from different directions by movement of the impression or the digitalization unit, the shadowing on the surface cannot be completely excluded.

In view of the presented scanning accuracy of digitalization units, the regular need of maintenance has to be considered [33]. Furthermore, the accuracy of the scans might be influenced by the specific optical scanning unit (scanning wands). For the present study, the current software version and one singular scanning wand was used, with an up-to-date calibration of the system. The use of the intraoral and desktop scanning devices was specially trained to ensure reliable data under study conditions. In further studies, the reproducibility of the obtained values has to be proven under the conditions of the daily clinical routine with different users, different scanning wands, and different software versions. Also, additional surveys must be performed to analyze if the high dataset accuracy can be transferred to a superior fit of a dental restoration over the complete manufacturing workflow.

Conclusions

Intraoral scanners are more and more used in daily routine; however, little is known about their accuracy when it comes to full-arch scans. Most current data are based on in vitro evaluations and do not represent the oral environment. This study compares for the first time an intraoral scan versus conventional impressions, in vitro versus in vivo, applying a new demonstrative methodology. The developed method seems

appropriate for in vivo analyses of the dimensional accuracy of full-arch digitalization. Under optimum conditions, the direct digitalization using the iTero Element intraoral scanning device results in the same and for single parameters even in higher accuracy than the indirect digitalization of the impression or the gypsum cast using a desktop scanner. For full-arch digitalization, the method of indirect digitalization of the impression itself resulted in lower accuracy than the indirect digitalization of the cast.

Funding The conduct of the present study was financially supported by Align Technology. Align Technology had no influence in the study design, nor in the collection, analysis, or interpretation of the data, nor in writing or submitting the publication.

Compliance with ethical standards

Conflict of interest The conduct of the present study was financially supported by Align Technology. Align Technology had no influence in the study design, nor in the collection, analysis, or interpretation of the data, nor in writing or submitting the publication.

Ethical approval This study was approved by the Ethics Committee (511-14) and registered at the German Clinical Trial Register (DRKS 00015459). All procedures performed in this study were in accordance with the ethical standards of the institutional and/or national research committee and with the 1964 Helsinki declaration and its later amendments or comparable ethical standards.

Informed consent Before starting the data acquisition, the voluntary patient signed an informed consent.

References

- Kuhr F, Schmidt A, Rehmann P, Wostmann B (2016) A new method for assessing the accuracy of full arch impressions in patients. *J Dent* 55:68–74. <https://doi.org/10.1016/j.jdent.2016.10.002>
- Edelhoff D, Schweiger J, Prandtner O, Trimpl J, Stimmelmayer M, Guth JF (2017) CAD/CAM splints for the functional and esthetic evaluation of newly defined occlusal dimensions. *Quintessence Int* 48(3):181–191. <https://doi.org/10.3290/j.qi.a37641>
- Edelhoff D, Beuer F, Schweiger J, Brix O, Stimmelmayer M, Guth JF (2012) CAD/CAM-generated high-density polymer restorations for the pretreatment of complex cases: a case report. *Quintessence Int* 43(6):457–467
- Güth JF, Almeida e Silva JSA, Beuer FF, Edelhoff D (2012) Enhancing the predictability of complex rehabilitation with a removable CAD/CAM-fabricated long-term provisional prosthesis: a clinical report. *J Prosthet Dent* 107(1):1–6. [https://doi.org/10.1016/S0022-3913\(11\)00171-5](https://doi.org/10.1016/S0022-3913(11)00171-5)
- Keul C, Stawarczyk B, Erdelt KJ, Beuer F, Edelhoff D, Guth JF (2014) Fit of 4-unit FDPs made of zirconia and CoCr-alloy after chairside and labside digitalization—a laboratory study. *Dent Mater* 30(4):400–407. <https://doi.org/10.1016/j.dental.2014.01.006>
- Ender A, Mehl A (2011) Full arch scans: conventional versus digital impressions—an in-vitro study. *Int J Comput Dent* 14(1):11–21
- Guth JF, Keul C, Stimmelmayer M, Beuer F, Edelhoff D (2013) Accuracy of digital models obtained by direct and indirect data capturing. *Clin Oral Investig* 17(4):1201–1208. <https://doi.org/10.1007/s00784-012-0795-0>

8. Guth JF, Edelhoff D, Schweiger J, Keul C (2016) A new method for the evaluation of the accuracy of full-arch digital impressions in vitro. *Clin Oral Investig* 20(7):1487–1494. <https://doi.org/10.1007/s00784-015-1626-x>
9. Mehl A, Ender A, Mormann W, Attin T (2009) Accuracy testing of a new intraoral 3D camera. *Int J Comput Dent* 12(1):11–28
10. Nedelcu RG, Persson AS (2014) Scanning accuracy and precision in 4 intraoral scanners: an in vitro comparison based on 3-dimensional analysis. *J Prosthet Dent* 112(6):1461–1471. <https://doi.org/10.1016/j.prosdent.2014.05.027>
11. Boeddinghaus M, Breloer ES, Rehmann P, Wostmann B (2015) Accuracy of single-tooth restorations based on intraoral digital and conventional impressions in patients. *Clin Oral Investig* 19(8):2027–2034. <https://doi.org/10.1007/s00784-015-1430-7>
12. Gimenez B, Ozcan M, Martinez-Rus F, Pradies G (2015) Accuracy of a digital impression system based on active wavefront sampling technology for implants considering operator experience, implant angulation, and depth. *Clin Implant Dent Relat Res* 17(Suppl 1):e54–e64. <https://doi.org/10.1111/cid.12124>
13. Gimenez B, Pradies G, Martinez-Rus F, Ozcan M (2015) Accuracy of two digital implant impression systems based on confocal microscopy with variations in customized software and clinical parameters. *Int J Oral Maxillofac Implants* 30(1):56–64. <https://doi.org/10.11607/jomi.3689>
14. Amin S, Weber HP, Finkelman M, El Rafie K, Kudara Y, Papaspyridakos P (2017) Digital vs. conventional full-arch implant impressions: a comparative study. *Clin Oral Implants Res* 28(11):1360–1367. <https://doi.org/10.1111/clr.12994>
15. Ciocca L, Meneghello R, Monaco C, Savio G, Sceda L, Gatto MR, Baldissara P (2018) In vitro assessment of the accuracy of digital impressions prepared using a single system for full-arch restorations on implants. *Int J Comput Assist Radiol Surg* 13:1097–1108. <https://doi.org/10.1007/s11548-018-1719-5>
16. Jeong ID, Lee JJ, Jeon JH, Kim JH, Kim HY, Kim WC (2016) Accuracy of complete-arch model using an intraoral video scanner: an in vitro study. *J Prosthet Dent* 115(6):755–759. <https://doi.org/10.1016/j.prosdent.2015.11.007>
17. Patzelt SB, Emmanouilidi A, Stampf S, Strub JR, Att W (2014) Accuracy of full-arch scans using intraoral scanners. *Clin Oral Investig* 18(6):1687–1694. <https://doi.org/10.1007/s00784-013-1132-y>
18. Ender A, Mehl A (2015) In-vitro evaluation of the accuracy of conventional and digital methods of obtaining full-arch dental impressions. *Quintessence Int* 46(1):9–17. <https://doi.org/10.3290/j.qi.a32244>
19. Ender A, Mehl A (2013) Accuracy of complete-arch dental impressions: a new method of measuring trueness and precision. *J Prosthet Dent* 109(2):121–128. [https://doi.org/10.1016/S0022-3913\(13\)60028-1](https://doi.org/10.1016/S0022-3913(13)60028-1)
20. Zimmermann M, Koller C, Rumetsch M, Ender A, Mehl A (2017) Precision of guided scanning procedures for full-arch digital impressions in vivo. *J Orofac Orthop* 78(6):466–471. <https://doi.org/10.1007/s00056-017-0103-3>
21. Flugge TV, Schlager S, Nelson K, Nahles S, Metzger MC (2013) Precision of intraoral digital dental impressions with iTero and extraoral digitization with the iTero and a model scanner. *Am J Orthod Dentofac Orthop* 144(3):471–478. <https://doi.org/10.1016/j.ajodo.2013.04.017>
22. Ender A, Attin T, Mehl A (2016) In vivo precision of conventional and digital methods of obtaining complete-arch dental impressions. *J Prosthet Dent* 115(3):313–320. <https://doi.org/10.1016/j.prosdent.2015.09.011>
23. Grunheid T, McCarthy SD, Larson BE (2014) Clinical use of a direct chairside oral scanner: an assessment of accuracy, time, and patient acceptance. *Am J Orthod Dentofac Orthop* 146(5):673–682. <https://doi.org/10.1016/j.ajodo.2014.07.023>
24. Accuracy (trueness and precision) of measurement methods and results—part 1: general principles and definitions (ISO 5725-1:1994)
25. Choi AH, Conway RC, Taraschi V, Ben-Nissan B (2015) Biomechanics and functional distortion of the human mandible. *J Investig Clin Dent* 6(4):241–251. <https://doi.org/10.1111/jicd.12112>
26. Sahin S, Cehreli MC (2001) The significance of passive framework fit in implant prosthodontics: current status. *Implant Dent* 10(2):85–92
27. van der Meer WJ, Andriessen FS, Wismeijer D, Ren Y (2012) Application of intra-oral dental scanners in the digital workflow of implantology. *PLoS One* 7(8):e43312. <https://doi.org/10.1371/journal.pone.0043312>
28. Wesemann C, Muallah J, Mah J, Bumann A (2017) Accuracy and efficiency of full-arch digitalization and 3D printing: a comparison between desktop model scanners, an intraoral scanner, a CBCT model scan, and stereolithographic 3D printing. *Quintessence Int* 48(1):41–50. <https://doi.org/10.3290/j.qi.a37130>
29. Muallah J, Wesemann C, Nowak R, Robben J, Mah J, Pospiech P, Bumann A (2017) Accuracy of full-arch scans using intraoral and extraoral scanners: an in vitro study using a new method of evaluation. *Int J Comput Dent* 20(2):151–164
30. Nowak R, Wesemann C, Robben J, Muallah J, Bumann A (2017) An in-vitro study comparing the accuracy of full-arch casts digitized with desktop scanners. *Quintessence Int* 20:667–676. <https://doi.org/10.3290/j.qi.a38676>
31. Persson AS, Oden A, Andersson M, Sandborgh-Englund G (2009) Digitization of simulated clinical dental impressions: virtual three-dimensional analysis of exactness. *Dent Mater* 25(7):929–936. <https://doi.org/10.1016/j.dental.2009.01.100>
32. Matta RE, Adler W, Wichmann M, Heckmann SM (2017) Accuracy of impression scanning compared with stone casts of implant impressions. *J Prosthet Dent* 117(4):507–512. <https://doi.org/10.1016/j.prosdent.2016.07.026>
33. Rehmann P, Sichwardt V, Wostmann B (2017) Intraoral scanning systems: need for maintenance. *Int J Prosthodont* 30(1):27–29. <https://doi.org/10.11607/ijp.4976>

Publisher's note Springer Nature remains neutral with regard to jurisdictional claims in published maps and institutional affiliations.